

HADLEY CENTRE
FOR CLIMATE PREDICTION AND RESEARCH

**Sea temperature bucket models
used to correct historical SST
data in the Meteorological Office.**

by

C. K. Folland

CRTN 14

September 1991

CLIMATE
RESEARCH
TECHNICAL
NOTE

Hadley Centre
Meteorological Office
London Road
Bracknell
Berkshire RG12 2SY

CLIMATE RESEARCH TECHNICAL NOTE No 14

MODELS OF THE COOLING OF SEA WATER BUCKETS USED TO CORRECT

HISTORICAL SEA SURFACE TEMPERATURE DATA

by

C K Folland

SEPT 1991

Hadley Centre for Climate Prediction and Research
Meteorological Office
London Road
Bracknell
Berkshire RG 12 2SY
UK

NOTE: This paper has not been published. Permission to quote from it should be obtained from the Director of the Hadley Centre

Abstract

The theory is presented of the physical models used to correct historical sea surface temperature (SST) data. The models calculate the rate of loss of heat from ocean water in a bucket during a measurement, assuming that the water is always well-mixed. Two types of models are considered: (a) uninsulated, soaked canvas bucket or highly conducting metal bucket with a wet surface, and (b) partly insulated wooden bucket. Full details of how the models are used to correct historical SST data are given in Folland and Parker (1990, 1992), henceforth FP, and in Parker and Folland (1991) (PF). Idealised examples are given of the cooling rates of water in the buckets when exposed on deck. Finally results of an initial set of field tests of the theory are given where the observed cooling of a canvas bucket on deck is compared with that predicted.

1. Introduction

Allowance has already been made in the observations section of the IPCC (1990) Science Report (Folland, Karl and Vinnikov, 1990) for the substantial influence on assessed climate change of the artificial cooling of observed sea surface temperature data before 1942 due to the widespread use of uninsulated buckets at that time. Both SST analyses used in the IPCC Science Report (Bottomley *et al.*, 1990 and Farmer *et al.*, 1989) were corrected by early versions of the theory discussed here. The "bucket" corrections have the effect of decreasing the apparent magnitude of long term SST changes, making them quite similar to those assessed for surface air temperatures over land. Climate changes independently measured over the oceans from ship's air temperatures also become similar. This note gives full details of the theory of the bucket models that contribute to the Bottomley *et al.* "refined" SST corrections and identifies recent improvements to the models. The way in which the models are used to calculate corrections to historic SST data is summarised in section 8.3; a fuller discussion appears in FP(1990).

Models of the heat exchange between uninsulated and partly insulated wooden buckets and the atmosphere are derived from appropriate heat transfer theory. Because model boundary conditions change during the integrations, models are integrated step-by-step and analytical solutions are not used as was done by Farmer *et al.* (1989) (FWJS). The canvas bucket model is shown to reduce to the theoretical equations for a cylindrical wet bulb thermometer (Appendix 2). Models for wet metal buckets are not distinguished, though differences do, in principle, exist. The model of the cooling of a wooden bucket is derived with the help of the primitive equation of unsteady heat transfer through a poorly conducting plane wall. It is shown that an assumption made by FWJS that the wooden walls of sea-buckets are effectively totally insulating may not be adequate.

Folland and Hsiung (1987) discussed corrections to SST measured using canvas sea-buckets. Their theory is derived differently, and less fully, than that discussed here, though their equations give quite similar results. Corrections for the use of canvas buckets published in Bottomley *et al.* (1990) are based on an earlier, slightly modified, version of the theory presented here.

Differences are pointed out in the text as the theory is developed. Corrections for wooden buckets in Bottomley *et al.* use a simplified method mentioned in the summary (section 9).

1.1 Note about physical constants

The variation of certain physical "constants" which change a little with temperature, pressure and sometimes humidity has been ignored. As far as possible their values have been chosen to be those appropriate (where relevant) to an air pressure of 1015mb, a temperature of 20°C and an atmospheric relative humidity of 75%. Some physical quantities which vary considerably over the range of temperatures observed at sea but whose variation only has second or third order effects on the cooling rate of buckets have also been regarded as constant. Thus the long-wave radiative heat transfer coefficient, which varies by over 30% in the temperature range 0-30°C, has been given a value appropriate to a mean bucket surface and air temperature of 20°C and a bucket emissivity of 95%. In most cases, empirical constants are only quoted to two significant figures and occasionally one. These choices often differ slightly from those used in existing publications (e.g. Bottomley *et al.*) which were not completely consistent in this regard, but the effects of the changes are small. Wherever the heat transfer coefficients used here differ from those used before, the reasons are explained. The overall effects of all changes on calculated bucket corrections are, at most, strong second order.

2. The Canvas Bucket - model geometry and assumed pattern of use on deck

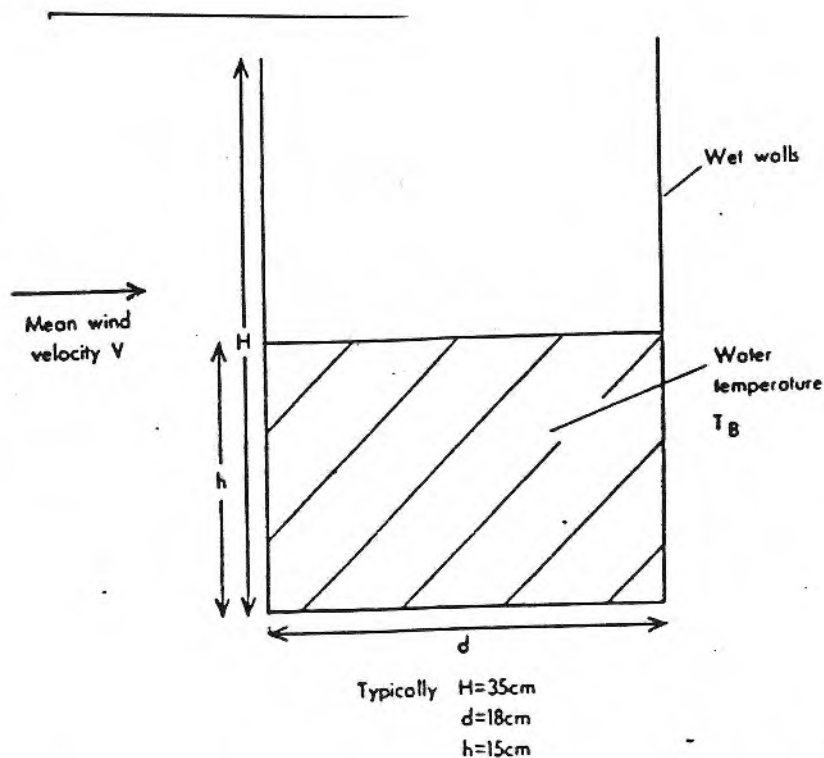


Figure 1 Conceptual diagram of a canvas bucket

Fig. 1 is adapted from FP(1990).

1. The top of the bucket may be open to the atmosphere but is regarded as effectively closed because the water surface is usually well below the rim, and so is exposed to a much lower than ambient average airflow speed (offset perhaps by increased mass and heat transfer due to extra turbulence inside the bucket entrance). In some buckets there may also be a lid. So although the entrance is shown open in Fig. 1, modelling is done for a closed bucket.

2. The bucket walls are assumed to freely evaporate at the potential rate while water in the bucket is assumed to be well-mixed and at the same temperature as the walls. The rate of cooling (or in rare cases, heating) of the bucket on deck is almost inversely proportional to the mass of water in the bucket for a fixed shape of bucket. So by choosing small and big buckets it is possible to change the cooling rate by a fairly large amount to determine the sensitivity of the corrections to bucket size (FP, 1990). In principle, the corrections are hardly affected if we integrate the model for a time almost proportional to bucket thermal capacity. The time for which the model is integrated is varied as briefly described in subsection 8.3 (discussed in detail in FP, 1990) where it is shown that the above procedure follows automatically during the calculation of corrections. Bucket shape can also be changed; in calculations done to date, only the ratio of bucket height to width has been changed, retaining a cylindrical shape. In reality bucket "height" is not defined by the physical height of the bucket walls but by the depth of water in the bucket. This arises because the thermal mass of bucket walls not in contact with the water are ignored. This is acceptable as heat transfer vertically within the walls is small, the walls being very thin.

3. The base of the bucket is assumed to freely evaporate at the same temperature as the water. For certain buckets this may not be true, e.g. the bucket described by Ashford (1948) and widely used by the Meteorological Office where the base is wooden. Here the wooden base contains holes which allow water to circulate underneath a thin metal plate placed above the wooden base, with a gap in between, which serves as an inner watertight base. Thus if the theory overestimates the cooling of water due to evaporation from the base of buckets in general, this is compensated by not allowing evaporation (or any other heat transfers) from the free water surface. This is discussed further in section 3.1.2.

4. A typical method of observing the SST can be summarised as follows (based on various sources: e.g. Brooks, 1926, Maury, 1858, Meteorological Office 1868, 1956). FP(1992) give a more complete list.

(a) The bucket (wooden or canvas) was lowered into the sea and left for a minute or longer to fill (a canvas bucket rarely fills completely).

(b) The bucket was carefully hauled over the ship's side and placed on deck, or hung from a suitable projection just above the deck. The rate of cooling of the bucket is slightly different between these two cases, the former situation inhibiting

evaporation from the bucket base. In canvas bucket models it is assumed that the bucket hangs freely as this is more convenient though instructions are generally silent on this.

(c) The thermometer was placed into the sea water contained in the bucket as soon as possible and allowed to come into equilibrium by stirring the water with the thermometer. Sometimes the thermometer bulb was protected by a shield (thermometer protector) incorporating a small water reservoir. We have included the small effect on the water temperature of inserting a thermometer initially at the dry bulb temperature into the water; this was not included by FWJS in their model. The thermometer and reservoir in all models discussed here are allocated a nominal (empty) combined thermal capacity of 35gm of water as described by Ashford (1948). Inclusion of this term usually has little effect and reduces as bucket volume increases, but is strong second order in winter in the Gulf Stream and Kuroshio current regions. The term was included because it seemed to be necessary to fully explain some experimental results of Brooks (1926) in the Gulf stream region.

(d) After an additional period varying from 1-2 minutes (typical in the twentieth century) to 4-5 minutes (Maury, 1858) the thermometer was read. This time is not assumed in the model, but as indicated above, is calculated from the time needed to create corrections that best equates the size of the annual cycle of SST data in pre-1942 data with that in 1951-80 in extratropical regions. This procedure would fail if the model were qualitatively inappropriate as the annual cycle of corrections must vary qualitatively in the correct manner, with larger corrections in winter. Sometimes the temperature was measured by first quickly extracting a thermometer with attached water reservoir from the bucket (Brooks, 1926). We have neglected extra cooling caused by this procedure as it may not have been general. When this happened, much faster cooling would often occur. It is likely that the influence of individual temperatures severely affected in this way will have been minimised by the quality control procedures of Bottomley et al.

An effect which concerned Brooks has been excluded. He carried out experiments to show that when a canvas bucket first entered the water it was generally cold relative to the SST, sometimes considerably so. Unless the bucket was trawled in the water for long enough, or was dipped into the sea twice, the first sample of water being thrown away, additional cooling of the sea water could result. On the other hand, if the bucket was taken inside the ship (erroneously) or stored in a place exposed to strong solar insolation, it might have entered the sea too warm. So we ignore any bias in the initial temperature of the canvas (or wood in section 6).

Note that climatological wind speeds are used in a special way to calculate corrections in Bottomley et al. which allows for the non-linear influence of wind speed on heat transfer. FP(1990) give details. On deck, the ambient wind speed is assumed to be less than during the bucket hauling phase; in both cases wind speeds are assumed to be substantially less than reported at 10m, as discussed later.

3. Theory of heat losses from uninsulated sea-buckets - introduction

A sea temperature bucket is regarded as an upright circular cylinder subjected to airflow transverse to its axis (Fig. 1). For buckets of usual dimensions, turbulent airflow around a bucket is "sub-critical" (Folland, 1988). Under these conditions, the flow around the bucket can be parameterised in a fairly straightforward way because the geometry of the flow remains quite "similar" for the observed range of Reynolds numbers, Re , ($1 < Re < 2 \times 10^5$) with minor modifications for $Re < 1000$. Eckert and Drake (1985) (ED, 1985) give details. The Reynolds number for a cylinder in transverse flow is given by:

$$Re = \frac{\bar{u}_0 D}{\nu} \quad (1a)$$

where \bar{u}_0 = mean freestream air velocity

D = cylinder (bucket) diameter

ν = kinematic viscosity of moist air (about $1.5 \times 10^{-5} \text{ m}^2 \text{ s}^{-1}$ at 20°C and "normal" pressure assuming an air density of 1.2 kg m^{-3} (Kaye and Laby, 1986)).

Now $\nu^{-1} = 67000 \text{ m}^{-2} \text{ s}$ (to two significant figures). Thus for all quantities in mks units:

$$Re = 67000 \bar{u}_0 D \quad (1b)$$

In general $0.05 < D < 0.2 \text{ m}$ for canvas or metal buckets (see FP, 1990).

Heat and mass transfer from typical buckets can be described with almost the same equations for $0.01 < u_0 < 20 \text{ ms}^{-1}$. "Calms" do not arise when the influence of the ship speed is taken into account (section 4). Fig. 2 (overleaf) shows the main components of heat transfer, taken from FP(1990):

a. Sensible heat exchange across the bucket and water surfaces (the latter may be small as discussed above and is ignored in the model derived here).

b. Evaporation from the wet canvas (metal) bucket surface and from the water surface in the bucket (the latter is assumed to be zero).

c. Long wave radiative heat exchange between the bucket, its inner water surface (this is ignored) and its surroundings.

d. Direct and diffuse short wave sky radiation and reflected radiation receipt by the bucket and its water surface. Reflected radiation is ignored, as is short wave radiation receipt by the water surface.

3.1 Sensible heat transfer rates

The sensible heat transfer coefficient between the bucket or water surface and the ambient air may vary systematically across its surface. A local sensible heat transfer coefficient h_{loc} is defined by:

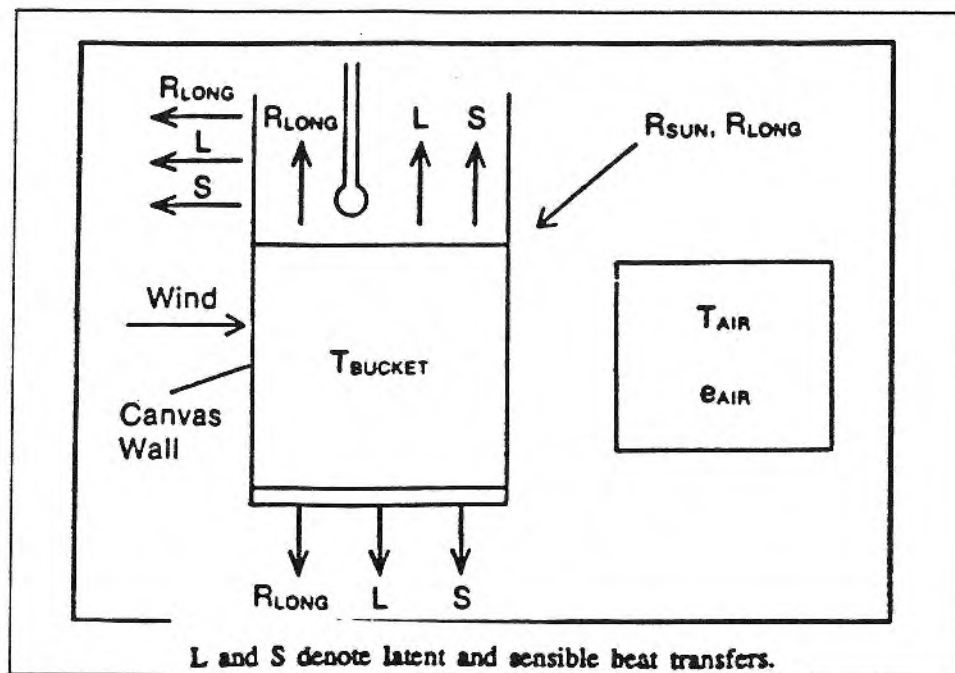


Figure 2 Heat transfers from an uninsulated bucket

$$\frac{dQ_s}{d\tau} = h_{loc} A (t_b - t_a) \quad (2)$$

Here $\frac{dQ_s}{d\tau}$ = local rate of transfer of sensible heat

A = local areal size of bucket

t_b = local temperature of bucket surface

t_a = ambient temperature of air (same everywhere)

where τ is used to denote time. Now h_{loc} can be re-expressed in terms of the local value of a dimensionless Nusselt number, Nu, for any geometry:

$$h_{loc} = \frac{k}{x} Nu_{loc} \quad (3a)$$

where k = thermal conductivity of air and x is the distance along the bucket surface from a reference position at its windward edge. Nu is nominally the ratio of x to the thickness Δ of the thermal boundary layer above the bucket surface, (ED, 1985 p176). Equation 3a results because h is defined to be the ratio k/Δ and heat transfer across the thin thermal boundary layer adjacent to

the bucket surface is considered to occur by conduction. The boundary layer is so thin that Nu is very large almost everywhere. For a bucket it is sufficient to calculate average values of h_{loc} and Nu_{loc} , i.e.

$$\bar{h} = \frac{k}{x} \overline{Nu} \quad (3b)$$

Henceforth Nu and h will represent average values.

3.1.1 Sensible heat transfer rate from the cylindrical sides

Eckert and Drake in their longer book on heat and mass transfer (Eckert and Drake, 1972) (ED, 1972) quote formulae for Nu_s given by Zhukauskas et al. (1968) for heat transfer from the external walls of (cylindrical) tubes in transverse flow (ED, p406). The formulae are expressed in terms of Re and another dimensionless quantity, the Prandtl number, Pr, of the air. The Prandtl number is the dynamic viscosity of air multiplied by its specific heat at constant pressure divided by its thermal conductivity or, equivalently, the ratio of the kinematic viscosity of the air and its thermal diffusivity. Simplified expressions for cylindrical geometry are:

$$Nu_{cyl} = 0.5Re^{0.5}Pr^{0.38} \quad (4a) \quad 1 < Re < 10^3$$

$$Nu_{cyl} = 0.25Re^{0.6}Pr^{0.38} \quad (4b) \quad 10^3 < Re < 2 \times 10^5$$

Equation 4a is essentially for flow around the bucket slower than the "sub-critical" turbulent range and equation 4b is for flow in that range. In equation 4a, a tiny constant term 0.43 added to $0.5Re^{0.5}$ by ED(1972) in their equation 9.29 (p406) has been neglected. A factor that multiplies both equations is also not explicitly shown: this is a function of the ratio of the Prandtl number of the free air to that at the cylinder walls and has been set to unity as suggested by ED. Equation 4 assumes that the reference value of x for a cylinder is taken to be (p 405 of ED, 1972):

$$\bar{x} = D$$

This is slightly different from the mean value of x measured between the windward and leeward-most points on the cylinder, $\pi D/4$. Substituting for Nu in equations 4a and 4b gives equations 5a and 5b:

$$h_{cyl} = 0.5k \left(\frac{\overline{u_0}}{\nu D} \right)^{0.5} Pr^{0.38} \quad (5a) \quad 1 < Re < 10^3$$

$$h_{cyl} = 0.25k \frac{\overline{u}_0^{0.6}}{v^{0.6}D^{0.4}} Pr^{0.38} \quad (5b) \quad 10^3 < Re < 2 \times 10^5$$

Substituting $Pr=0.71$, $v=1.5 \times 10^{-5} \text{m}^2\text{s}^{-1}$ and $k=0.025 \text{Wm}^{-1} \text{ } ^\circ\text{C}^{-1}$, gives:

$$h_{cyl} = 2.8 \left(\frac{\overline{u}_0}{D} \right)^{0.5} \quad (5c) \quad 1 < Re < 10^3$$

$$h_{cyl} = 4.3 \frac{\overline{u}_0^{0.6}}{D^{0.4}} \quad (5d) \quad 10^3 < Re < 2 \times 10^5$$

Equations 5c and 5d do not properly allow for turbulence in the incident flow. If this exists, as is likely on a ship, the heat transfer coefficients may on average be somewhat larger. In previous work trivially different heat transfer coefficients from those used here of 2.9 and 4.5 were used.

3.1.2 Sensible heat transfer rate from the base

No readily available formula was found, so one was derived. ED, 1985, p176, give the local Nusselt number for heat transfer from a flat plate subject to forced convection in laminar flow:

$$Nu_x = \frac{h_x x}{k} = 0.33 (Re_x)^{0.5} Pr^{0.333} \quad (6a)$$

$$\text{remembering that } Re_x = \frac{\overline{u}_0 x}{v}$$

Because the plate or base is nominally flat, the laminar flow formulation is reasonable (but see below). From this the average heat transfer coefficient for the base, regarded as a circular flat plate, is calculated from geometrical considerations. Appendix 1 gives:

$$h_{base} = 4.3 \left(\frac{\overline{u}_0}{D} \right)^{0.5} \quad (6b)$$

This formula is approximate in practice as a real bucket base may have a complicated structure, as for the Ashford (UK Met Office) canvas bucket. The bucket may also swing in the wind and increase the base heat transfer coefficient. On the other hand the rope used to suspend the bucket may cover part of the base and decrease heat exchanges. Overall, equation 6b seems adequate, as the influence of the base on heat transfers is usually markedly

less than for the cylindrical walls because of its smaller area. In previous work a smaller heat transfer coefficient of 2.8 was used (0.65x4.3) to allow for the influence of a rope around the base. This is not now felt to be justified given the neglect of possible heat transfers from the top of the bucket.

The difficulty about deciding on the efficiency of cooling from the base of an Ashford (Met Office) type canvas bucket was resolved as follows. The cooling rate of the base was multiplied by factors F in the range $0 < F < 2$ (F=2 assumes unrestricted heat transfer from the base and the water surface) and the calculated cooling after 1 minute was compared with that observed in a wind tunnel by Ashford (1948). His observations were made over a wide range of differences between the bucket temperature and the wet bulb temperature (see FP, 1990). Use of F=1 with the model derived above gave an almost perfect agreement with observation in all conditions, even better than for the similar calculation in FP(1990). Details will be given in FP(1992). So the base is assumed to freely evaporate. (Note that wind tunnel airflows are not usually turbulent). Real heat losses from the base are probably a little less than this but are compensated by small heat losses from the water surface and possibly by slightly larger heat transfer coefficients than assumed because of turbulence in the incident flow. The diagrams in section 7 assume F=.25 so bucket cooling rates are a little less than for F=1.

3.1.3 Sensible heat transfer from the upper water surface

This is likely to be small because the upper water surface is usually well within the bucket and some buckets have lids. The use of F=1 in section 3.1.2 which automatically excludes sensible heat losses from the open water surface for a canvas bucket is therefore adequate. However, they are included in wooden bucket models because these probably had no lids and may also have filled with sea water more successfully (section 6).

3.1.4 Total sensible heat transfers

Let the area of the bucket side (cylindrical) walls be A_{cyl} and that of the base be A_{base} . Then the total rate of loss of heat due to sensible heat transfer is:

$$\frac{dQ_s}{dt} = (h_{cyl}A_{cyl} + h_{base}S_{base}) (t_b - t_a) \quad (7)$$

3.2 Evaporative heat transfer rates

Evaporative heat transfer calculations involve intermediate calculations of mass transfer from the bucket surface to the air. The equations used to calculate mass transfers associated with evaporation are similar to those used in sensible heat transfer. The main change is that the local Nusselt number is replaced by a local Sherwood number, Sh, (ED, 1972, p732) defined by:

$$Sh_x = \frac{h_m x}{C_m}$$

where h_m is the mass transfer coefficient and C_m the mass diffusion coefficient. For a flat plate (bucket base) evaporating in forced laminar flow, an equation similar in form to equation 6a for sensible heat transfer is obtained:

$$Sh = 0.33Re_x^{0.5}Sc^{0.333}$$

Sc is the Schmidt number, the ratio of the kinematic viscosity to the mass diffusion coefficient. This equation is valid for values of $Sc > 0.6$ appropriate to the bucket situation. ED (1985) indicate (p476) that for the evaporation of water into air, the ratio of the thermal diffusivity to the mass diffusion coefficient at 20°C is 0.835. Manipulation of the above equation for Sh and equation 6a gives:

$$Sc = 0.835Pr \quad \text{and} \quad h_m = 1.13 \frac{h}{\rho_a c_p}$$

where ρ_a is the density of moist air, c_p is the specific heat of air at constant pressure and h is, as before, the sensible heat transfer coefficient. Thus equations for h_m are similar to those for h . In previous work (Bottomley et al.) it was assumed that $Pr = Sc$.

3.2.1 Replacing h_m by a function of h

The appropriate form of the evaporative heat transfer equation for the base and cylindrical walls of the canvas bucket can be derived from the equations for mass transfer as below. It is shown that the sensible heat transfer coefficients already derived for the base and cylindrical walls can be retained if an extra term is incorporated for evaporative heat losses. The mass transfer coefficient is defined from:

$$\frac{dm}{dt} = h_m (m_b - m_a) \quad (8a)$$

where m is the mass fraction of the vapour in the moist air so that m_b and m_a are mass fractions in the air at the bucket surface and in the free atmosphere respectively. Equation 8a relates to mass transfer per unit area. Using the identities in the previous paragraph we can substitute h for h_m :

$$\rho_a \frac{dm}{dt} = 1.13 \frac{h}{c_p} (m_b - m_a) \quad (8b)$$

Now $m = \frac{\rho_w}{\rho_a}$ the ratio of the density of water vapour and air.

Regarding the density of air as constant:

$$\frac{d\rho_w}{d\tau} = 1.13 \frac{h}{c_p \rho_a} (\rho_{wb} - \rho_{wa}) \quad (8c)$$

Let L be the latent heat of evaporation. The rate of loss of heat per unit volume associated with the evaporation of a given amount of water vapour is then:

$$\frac{dQ_w}{d\tau} = \frac{d}{d\tau} (\rho_w L)$$

Thus from (8c)
$$\frac{dQ_w}{d\tau} = 1.13 \frac{hL}{c_p \rho_a} (\rho_{wb} - \rho_{wa})$$

From the gas laws:

$$\rho_w = \frac{eM_w}{RT} \quad \text{and} \quad \rho_a = \frac{pM_a}{RT}$$

M_w is the molecular weight of water vapour, M_a that of air, R the universal gas constant, T the absolute temperature, p the atmospheric pressure and e the vapour pressure. Taking the ratio of these quantities with $M_w/M_a=0.62$, the rate of heat transfer associated with evaporation expressed as a function of h is:

$$\frac{dQ_w}{d\tau} = 0.70 \frac{hL}{pc_p} (e_b - e_a)$$

Expressing e_b and e_a in mb, and setting $L=2.45 \times 10^3 \text{ J Kg}^{-1}$, $p=1015 \text{ mb}$ and c_p for air $=10^3 \text{ J Kg}^{-1} \text{ }^\circ\text{C}^{-1}$, the rate of loss of heat per unit area becomes:

$$\frac{dQ_w}{d\tau} = 1.7h(e_b - e_a) \quad (9)$$

The bucket surface vapour pressure should be that of sea water the vapour pressures of pure water appropriate to the bucket surface (but not the air) are multiplied by 0.98. Evaporation may be even less if salinity tends to increase on the bucket surface, though diffusion of water from inside the bucket should minimise this. Note that the factor 1.7 in equation 9 was previously set to 1.5 because Pr was set equal to Sc.

3.3 Total rate of heat lost by sensible and evaporative mechanisms

This is given by:

$$\frac{dQ}{d\tau} = \frac{dQ_s}{d\tau} + \frac{dQ_w}{d\tau} \quad (10a)$$

Thus from (7) and (9) $\frac{dQ}{d\tau} = (h_{cyl} A_{cyl} + h_{base} A_{base}) (t_b - t_a + 1.7 (e_b -$

3.4 Heat transfers by long-wave radiation

Assuming the emissivity is unity, let the rate of emission of long wave radiation per unit area from the bucket be H_b and the rate of reception from its surroundings, assumed to be at the air temperature, be H_a . Then the net heat lost by the bucket due to long wave radiative heat transfer is:-

$$H_b - H_a = \sigma (t_b^4 - t_a^4) \approx 4\sigma \left(\frac{t_b + t_a}{2} \right)^3 (t_b - t_a)$$

The long wave radiative heat transfer coefficient is defined as:

$$h_r = 4\sigma \left(\frac{t_b + t_a}{2} \right)^3$$

The value of h_r varies markedly with temperature but, because it is a small factor in the heat budget of buckets, a fixed value of $5.4 \text{ Wm}^{-2} \text{ }^\circ\text{C}^{-1}$ has been used (appropriate for an average of the bucket surface and the air temperature of 20°C). The total effective area of the bucket exchanging long wave radiation with the surroundings is that of the sides and the base, exchanges from the water surface being neglected. The total net loss of heat due to long wave radiation is then:

$$\frac{dQ_l}{d\tau} = h_r (A_{base} + A_{cyl}) (t_b - t_a) \quad (11)$$

3.5 Total heat transfer rate by sensible, evaporative and long wave mechanisms

Expressed as the rate of heat loss from the bucket, this is given by adding equations 10b and 11 to give equation 12:

$$\frac{dQ}{d\tau} = h_r (A_{base} + A_{cyl}) (t_b - t_a) + (h_{cyl} A_{cyl} + h_{base} A_{base}) [t_b - t_a + 1.7 (e_b - e_a)]$$

3.6. Influence of solar radiation

This section is modified from that in Folland and Hsiung (1987) (FH). By day the influence of incident short wave radiation needs to be accounted for. In the current correction procedure this is derived from 24 hour monthly climatological averages of incident

short wave radiation intensity Q_s actually absorbed by a local horizontal ocean surface and varies with latitude, longitude and season. Section 3.6 derives the 24 hour average intensity incident on the bucket. $Q_s=0$ is assumed for the base, so Q_s only affects the bucket walls.

3.6.1 Calculation of Q_s

Let the albedo of the ocean be a (set to a constant value of 0.06). Then the radiation intensity incident on unit area of a horizontal ocean surface is:

$$Q_{so} = \frac{Q_s}{(1-a)}$$

The component of this radiation normal to a vertical bucket surface is easily shown to be, where θ is the angle of incidence of the radiation to the horizontal:

$$Q_{sn} = \frac{Q_{so}}{\tan\theta} \text{ or } \frac{Q_s}{(1-a)\tan\theta}$$

The radiation intensity varies around the bucket, some of the bucket being in shade. Its average depends on θ . If the albedo of off-white canvas=0.2, an initial estimate of mean intensity is:

$$Q_{s1} = 0.8 \frac{Q}{\pi(1-a)\tan\theta}$$

In FH, Q_{s1} was scaled by the ratio of the whole active surface area of the bucket (base+sides) to the area of the sides alone for computational convenience. Now θ varies with latitude and season. This was not allowed for in FH or in the programs used to calculate idealised bucket cooling curves in section 7 but was allowed for in Bottomley *et al.* The proportion of full sky radiation considered diffuse has been set to one third with a geometrically calculated mean angle of incidence of 33° (35° used in FH). In this note an average effective diurnal mean angle of combined diffuse and direct radiation θ_m of $\theta_m=35^\circ$ is assumed giving $\tan \theta_m=0.7$. This gives:

$$Q_{s2} = 0.4Q_s \quad (13a)$$

This simplified formula will not be used in revisions to the correction procedure. There is of course doubt about the extent to which buckets were in shade or in the sun; the influence of Q_s depends on how much care was taken to keep buckets in the shade. Fortunately the influence of Q_s is small, though not always quite negligible (see section 7 for examples of its influence).

3.6.2 Bucket equation with solar radiation

Inserting the simplified factor for solar radiation and noting that it represents a heat gain:

$$\frac{dQ}{d\tau} = h_r (A_{base} + A_{cyl}) (t_b - t_a) + (h_{cyl} A_{cyl} + h_{base} A_{base}) [t_b - t_a + 1.7 (e_b - e_a)] - 0.4$$

4. Overall change in bucket temperature

The change in bucket temperature due to all the above processes in unit time interval (one second) is given by:

$$\frac{dt_b}{d\tau} = \frac{1}{w_b c_b + w_w c_w} \frac{dQ}{d\tau} \quad (13c)$$

where w_b and c_b are the mass and specific heat of the bucket material (these might be different for the base and the sides) and w_w and c_w are corresponding parameters for sea water.

4.1 Influence of inserted thermometer on heat transfer rate and water temperature

The canvas bucket models are integrated in half minute steps (FP, 1990) and a thermometer inserted into the bucket at the third step. All heat exchanges between the thermometer and the water in the bucket are assumed to take place in the third half minute. The thermal capacity of the thermometer and its "protector" is set equal to the equivalent of 35gm of water as described by Ashford (1948). Thus in the third half minute the rate of heat transfer (per second) is increased temporarily:

$$\frac{dQ_{th}}{d\tau} = \frac{dQ}{d\tau} + 0.0012 (t_b - t_a) \quad (14a)$$

The factor 0.0012 represents a nominally uniform rate of exchange of heat between the thermometer and the water in the bucket in each second in the third half minute. Temperature changes in the third and subsequent half minutes are given by equations 14b and 14c respectively:

$$\frac{dt_b}{d\tau} = \frac{1}{w_b c_b + w_w c_w + 0.035} \frac{dQ_{th}}{d\tau} \quad (14b)$$

$$\frac{dt_b}{d\tau} = \frac{1}{w_b c_b + w_w c_w + 0.035} \frac{dQ}{d\tau} \quad (14b)$$

5. Allowance for ship speed

In the uninsulated and wooden bucket models an allowance is made for a mean ship speed, partly derived from an investigation of log books. The assumed mean ship speed varies from 4ms^{-1} in the mid-nineteenth century to 7ms^{-1} in 1940. It is combined with the climatological wind speed to obtain a representative wind speed around the bucket. However both speeds are reduced to allow for the sheltering influence of the ship and the height of the bucket above the sea. Different assumptions about this reduction have been made (FP, 1990) but typical examples are: hauling phase: a reduction factor of 0.6 for the ambient wind speed but unity for ship speed; on deck: a reduction factor of 0.4 for the ambient wind and 0.5 (in this note) or 0.67 (in some models) for ship speed. Ship speed has the largest effect in the lightest winds. The method is as follows:

Let the reduced climatological wind speed past the bucket be u , the reduced ship speed be s and the angle between the ship's heading and the ambient wind vector be θ . The angle can be any value so we assume a uniform distribution of angles and calculate an average vector combination of the two reduced speeds, u' from:

$$u' = \frac{1}{2\pi} \int_0^{2\pi} [(u^2 - 2usc\cos\theta + s^2)^{0.5}] d\theta = (u^2 + s^2)^{0.5} \quad (15)$$

The right hand side of this equation is approximate and typically overestimates the wind speed by about 5%. This error is small compared to uncertainties in the assumptions about the actual wind speed around a bucket on a ship's deck. So if the ship speed is 4ms^{-1} and the wind speed is zero, equation 15 gives $u' = 2\text{ms}^{-1}$ for a ship speed reduction factor of 0.5.

6. The wooden bucket model

Observational procedures for wooden and canvas sea buckets are assumed to have been qualitatively the same. A nineteenth century oak bucket covered in iron bands and used on a ship has been found (Parker, personal communication) though there is no indication that it was used for taking sea temperatures. This bucket had sides $\frac{1}{4}$ " (1 cm) thick and on average was 10" in diameter, wider at the top than the bottom. This bucket would probably have filled quite easily - and the water surface would have been open to the atmosphere. So it is assumed that the water surface exchanged heat quite freely with the environment. Also the volume of water collected in wooden buckets may have been markedly more than in canvas ones. Fig. 3 shows the wooden bucket as modelled.

The main assumptions are:

1. The open surface of the water is fairly near the top of the bucket. Thus sensible and evaporative heat transfers will occur and solar radiation will affect the surface.
2. The external bucket walls will be wet on leaving the ocean.

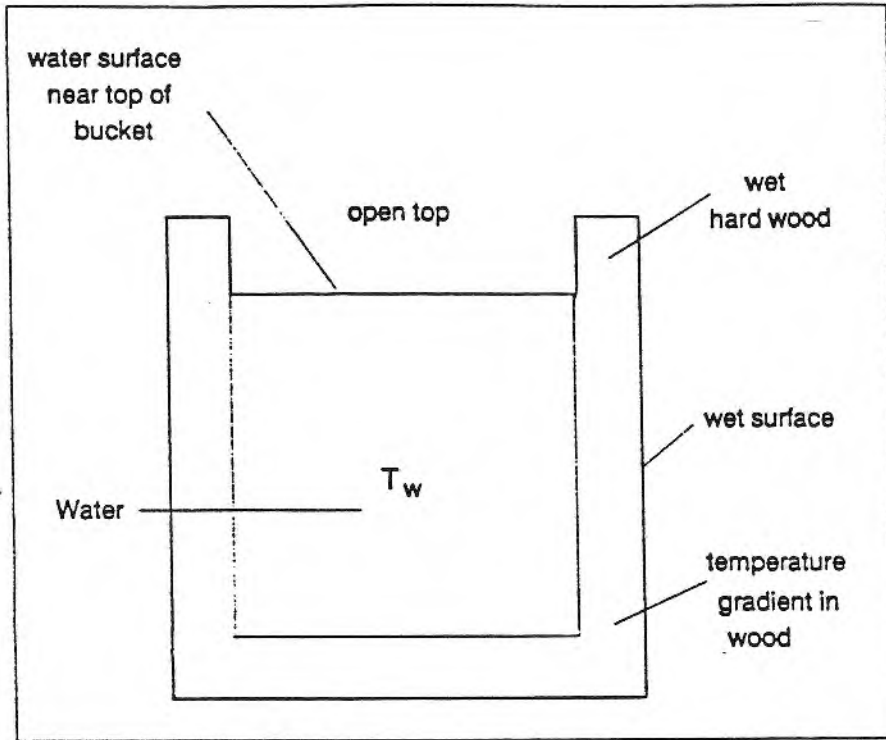


Figure 3 Conceptual model of a wooden bucket

The wood of the bucket walls should also be damp from frequent immersion. Because bucket walls are made of many pieces of wood, as in a barrel, there is a relatively large exposed surface area that can soak up water.

3. The walls are highly but not perfectly insulating. During exposure to the atmosphere a temperature gradient develops within the wooden walls which may be non-linear. Thus the outer surface of the wood can be at a markedly different temperature from the water inside the bucket. The set of heat transfer coefficients between the wood surface and the air is assumed to be the same as for the canvas bucket as the geometry is similar, ignoring the fact that a wooden bucket is not quite cylindrical. The three areas of heat exchange with the atmosphere are from:

- a. the water surface
- b. the bucket sides
- c. the bucket base

6.1 Rate of exchange of heat from the free water surface

It is assumed that the free water surface is exposed to the ambient airflow and solar radiation. However there will be some sheltering of the water surface that will reduce the airflow and cause shading of the water surface, effects that work in opposite directions but may not cancel. The heat transfer coefficient of the free water surface has been chosen as that appropriate to the bucket base multiplied by a factor ≤ 1 .

Referring to equation 13b for the canvas bucket, the rate of loss

of heat from the free water surface is obtained by retaining the terms in h_{base} only. Now Q_s was defined to be the short wave radiation penetrating the horizontal ocean surface. Q_s is thus appropriate to the flat water surface in the bucket without modification.

$$\frac{dQ}{dt} = A_{base} [(h_r(t_b - t_a) + h_{base}(t_b - t_a + 1.7(e_b - e_a)) - Q_s)] \quad (16)$$

Because of the uncertainty in the level of the water in wooden buckets a second versions of equation 16 has been used in recent correction procedures where all heat exchanges across the free water surface have been multiplied by 0.5. For sensible and latent heat exchanges, this is approximately the same as reducing the mean air velocity over the free water surface to 25% of that on the external walls.

6.2 Rate of heat exchange from wooden walls and base

Wooden buckets are assumed to be cylindrical so that the heat transfer coefficients associated with a cylindrical body in transverse flow can be used. The cooling of water in a bucket via heat exchanges through walls of finite thermal conductivity is a problem in unsteady heat transfer with variable boundary conditions. The simplest way of carrying out the calculations is to assume that the internal and external bucket surfaces are locally flat and parallel. This avoids the need to calculate heat flux divergences associated with the nominally larger cross-sectional area of the outside compared to the inside walls. For a typical wooden bucket with a mean diameter 25cm and wall thicknesses around 1-1.5cm, this assumption is excellent. It is also assumed that the flux of heat is one dimensional, i.e. directly from the water to the outside air with no fluxes vertically or sideways within the walls. The general equation for unsteady heat conduction is given by ED, 1985, p31. For one dimensional heat transfer in the x direction in a body with no internal heat source:

$$\frac{\partial t}{\partial \tau} = \frac{k}{\rho c} \frac{\partial^2 t}{\partial x^2} \quad (17a)$$

where t =temperature, τ is time and c is the specific heat. The factor $k/\rho c$ is the thermal diffusivity α . Equation 17a can be written in finite difference form:

$$\frac{\Delta_\tau t}{\Delta \tau} = \alpha \frac{\Delta_x^2 t}{(\Delta x)^2} \quad (17b)$$

The subscripts τ and x correspond to variable times and locations as equation 17b is a partial differential equation. Let a fixed place in the wall be n and a fixed time be p . Then equation 17b can be expanded to:

$$t_{n,p+1} - t_{n,p} = \alpha \frac{\Delta \tau}{(\Delta x)^2} (t_{n+1,p} - 2t_{n,p} + t_{n-1,p}) \quad (18)$$

Equation 18 is solved iteratively by dividing the bucket wall and base into layers of equal thickness as in Fig. 4. Five layers have been used in the model; experiments with three layers showed that cooling was more than 10% overestimated due to numerical errors even with very tiny time steps.

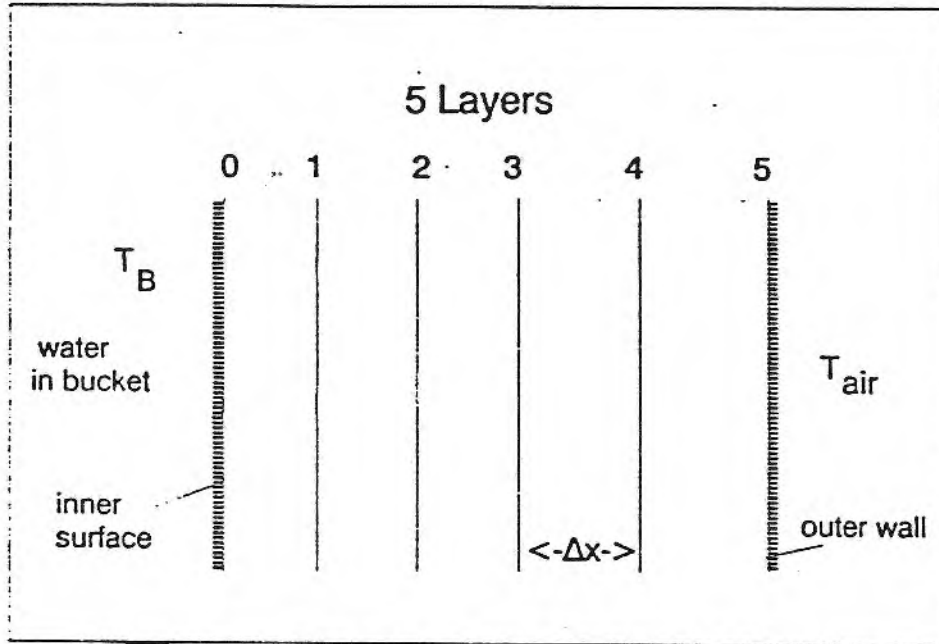


Figure 4 Division of bucket walls into five layers in the model

The temperature of all elements in Fig. 1 is initially set to the sea temperature. Experiments for a bucket wall and base thickness of 1 cm, thermal conductivity of wet oak $0.3 \text{ Wm}^{-1} \text{ }^{\circ}\text{C}^{-1}$, wet oak density 800 Kg m^{-3} and specific heat $1900 \text{ JKg}^{-1} \text{ }^{\circ}\text{C}^{-1}$ showed that a time step of 2 seconds with 5 layers gave on average errors (overestimates of heat transfer) of about 5% or less compared to the use of 10 layers and a time step of 0.05 seconds. This was regarded as satisfactory. The calculation proceeded as follows:

1. The heat loss from the exposed water surface, dQ_{top} , was calculated from equation 16. This gives an initial change to the water temperature and therefore that at $n=0$ in Fig. 4.

2. Heat fluxes in the cylinder wall and the base were calculated from the linear thermal conduction equation for the internal surface of the wall in contact with the water, and the internal surface of the base. The latter position, $n=0$, was assumed always to be at the water temperature. Thus the rate of loss of heat by the water in the bucket through the bucket wall and base is:

$$\frac{dQ_{cyl}}{dt} = kA_{cyl} \frac{(t_{0,p} - t_{1,p})}{\Delta x} \quad (19a)$$

$$\frac{dQ_{base}}{dt} = kA_{base} \frac{(t_{0,p} - t_{1,p})}{\Delta x} \quad (19b)$$

where Δx is the thickness of one layer, nominally that between $n=0$ and $n=1$.

3. The change of temperature at each point in the bucket wall and the base was calculated using equations like equation 18. Initially the outer surface ($n=5$) was set at the sea temperature. Calculations of the temperatures at other layer positions started at $n=4$ and proceeded iteratively to $n=1$.

4. The temperatures of the bucket wall and base surfaces were then changed using:

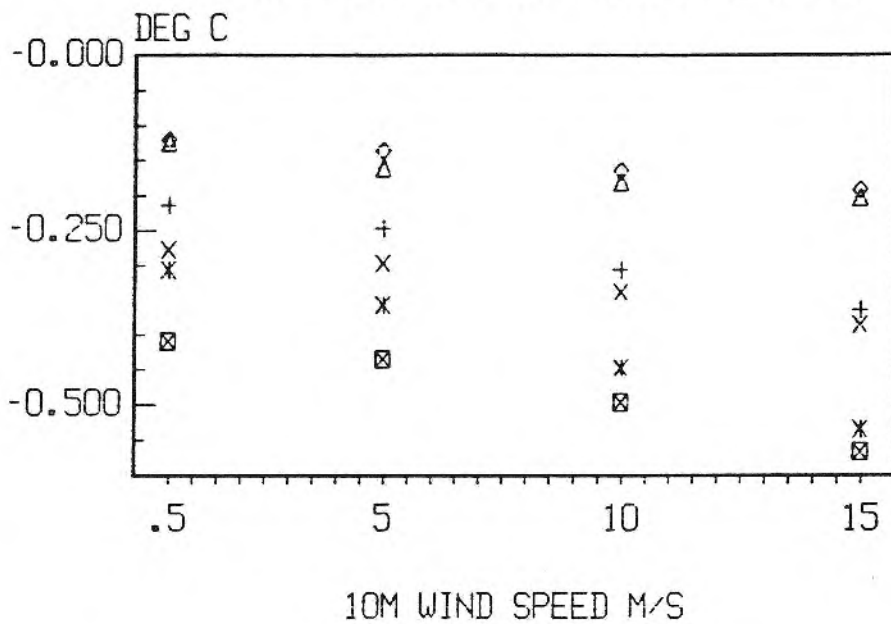
$$\frac{dt}{dt} = \frac{A_{cyl}}{M_{wcyl}} (0.4Q_s + h_r(t_a - t_{5,p}) + h_{scyl}[t_a - t_{5,p} + 1.7(e_a - e_{5,p})] + k \frac{(t_{4,p} - t_{5,p})}{\Delta x})$$

$$\frac{dt}{dt} = \frac{A_{base}}{M_{wbase}} (h_r(t_a - t_{5,p}) + h_{scyl}[t_a - t_{5,p} + 1.7(e_a - e_{5,p})] + k \frac{(t_{4,p} - t_{5,p})}{\Delta x})$$

M_{wcyl} and M_{wbase} are the products of the mass and specific heat of the water film on the two bucket surfaces (see next paragraph). It is unclear whether wooden buckets always stood on deck or were sometimes hung from a hook. It is assumed in correction procedures (but not in the examples in section 7) that wooden buckets were stood on deck (canvas buckets were assumed to hang free) and that heat transfer through the base ceased after hauling. Thus equation 20b is set to zero from the third half minute in correction procedures.

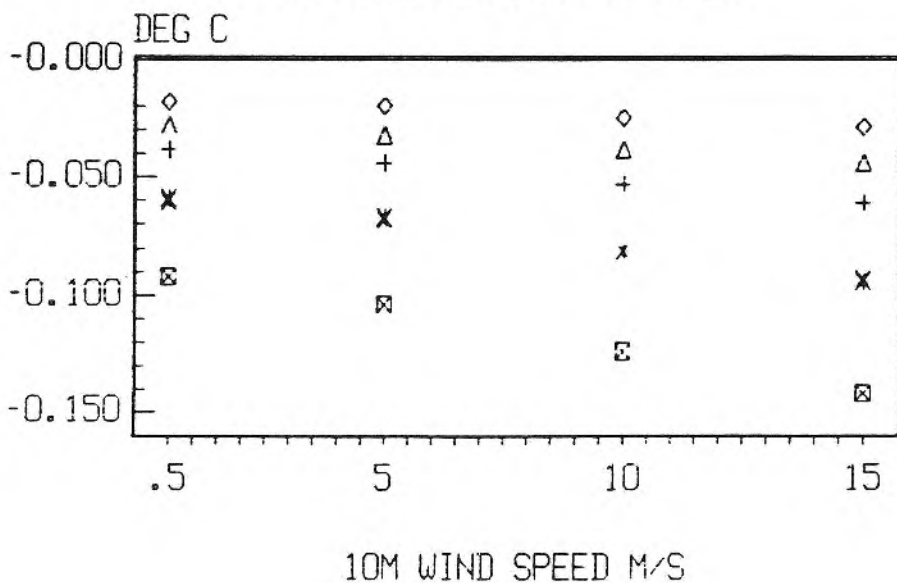
It was not initially clear whether a wooden bucket would retain a film of water on its outer surface for the duration of an observation. Experiments on small pieces of wet oak and softwood dipped into water, shaken and reweighed on a precision balance, showed that this water film thickness was initially about 0.1mm. Special runs of the model suggested that a film of this thickness would rarely disappear during the typical lengths of time for which the wooden bucket model needed to be integrated (up to 15 minutes for a very large bucket). So a constant film thickness of 0.1mm has been assumed for simplicity. The results are insensitive to other reasonable choices of thickness, or to decreasing the thickness as evaporation occurs, as long as a free water surface exists on the outside of the bucket that allows evaporative cooling to continue at the potential rate. Seepage of water through the wood and through the joints in the bucket is likely to have contributed to the maintenance of a water film

FIG 7 MODELLED COOLING OF LARGE CANVAS
 BUCKET AFTER 4 MINUTES
 SST=10 DEG C, AIR TEMPERATURE 8 DEG C



- ⊠ S=7 m/s
RH=50%
- * S=4 m/s
RH=50%
- × S=7 m/s
RH=75%
- + S=4 m/s
RH=75%
- △ S=7 m/s
RH=100%
- ◇ S=4 m/s
RH=100%

FIG 8 MODELLED COOLING OF LARGE WOODEN
 BUCKET AFTER 4 MINUTES
 SST=10 DEG C, AIR TEMPERATURE=8 DEG C
 (K in units of W/m²/degC)



- ⊠ K=.3
RH=50%
- * K=.15
RH=50%
- × K=.3
RH=75%
- + K=.15
RH=75%
- △ K=.3
RH=100%
- ◇ K=.15
RH=100%

FIG 9 MODELLED COOLING OF LARGE CANVAS
 BUCKET WITH INCREASING EXPOSURE TIME
 SHIP SPEED 7 M/S, RH=75%.

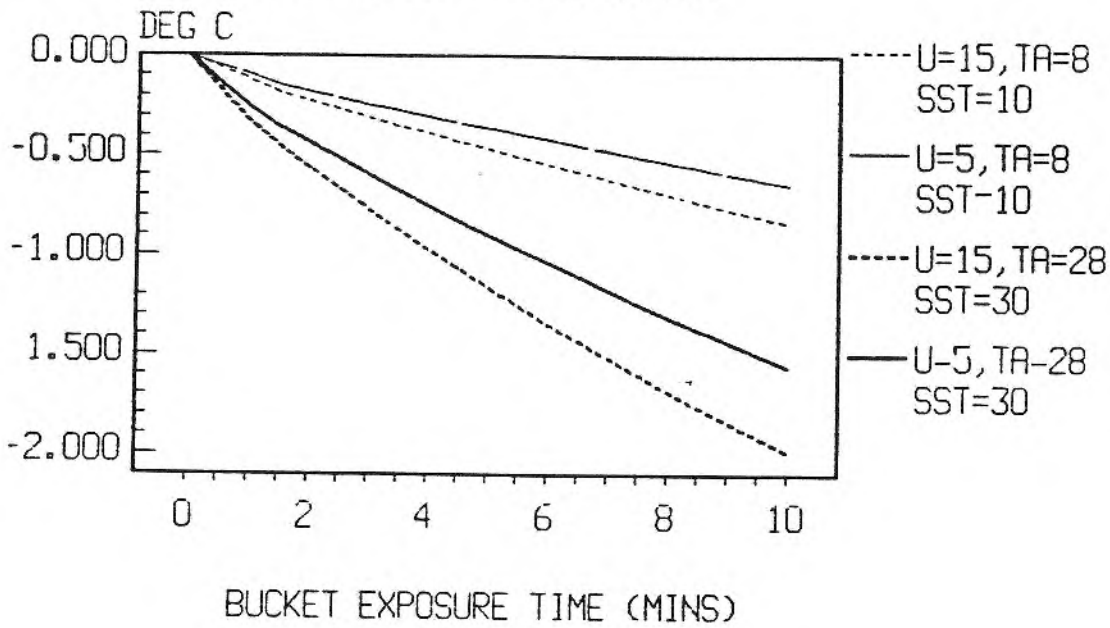


FIG 10 MODELLED COOLING OF LARGE CANVAS
 BUCKET-INFLUENCE OF SOLAR RADIATION

A U=5m/s SST=30, TA=28 deg C RH=75%
 B U=5m/s SST=10, TA=8 deg C RH=75%

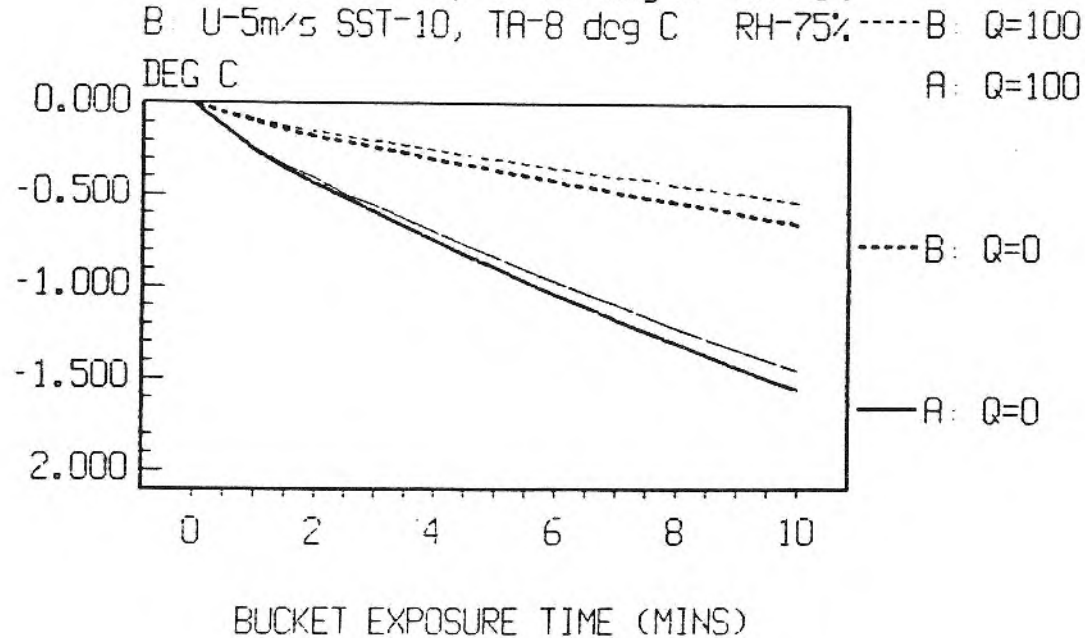
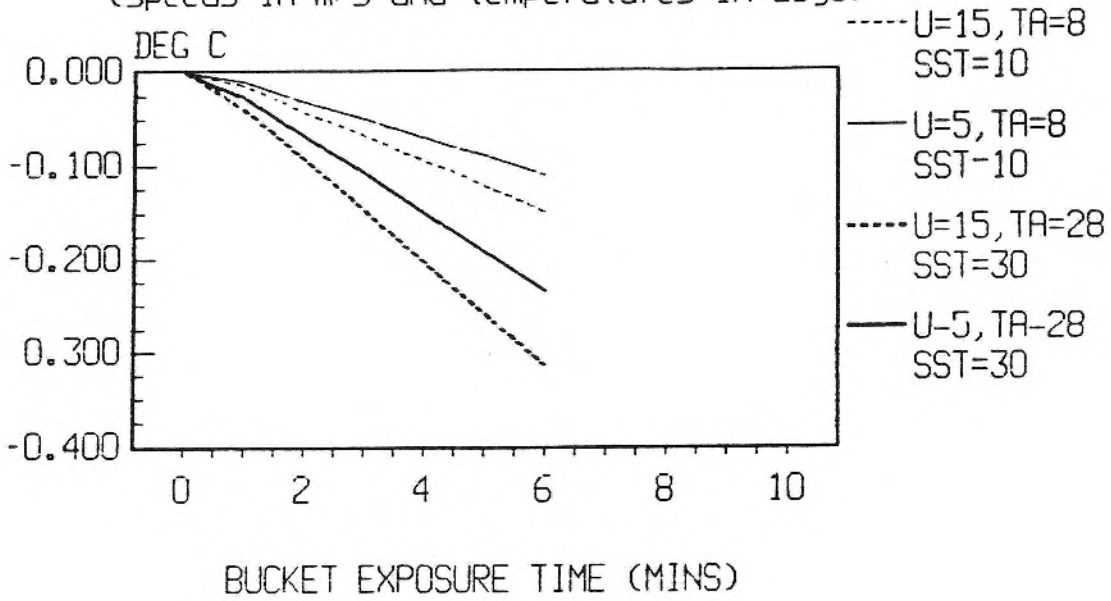


FIG 11 MODELLED COOLING OF LARGE WOODEN
BUCKET WITH INCREASING EXPOSURE TIME
(RH=75%, S=4, K=.3, wall thickness=1cm)
(speeds in m/s and temperatures in degC)



winds. Cooling also depends quite sensitively on air-sea temperature difference.

For a more typical equatorial air-sea temperature difference of -1°C , cooling would be reduced by 20-25% below the values in Fig. 5. Thus in equatorial regions with a relative humidity of 75%, $S=7\text{m/s}$, a 10m wind speed of 5m/s and an air-sea temperature difference of -1°C , typical modelled cooling of this large bucket after 4 minutes would still be rather over 0.5°C .

Fig. 6 shows similar cooling curves for the large wooden bucket (containing 10 litres of water) of wall thickness 1cm and thermal conductivities K (of wet oak) $0.3\text{ Wm}^{-1}\text{ }^{\circ}\text{C}^{-1}$ and $0.15\text{ Wm}^{-1}\text{ }^{\circ}\text{C}^{-1}$. The integration was done in 2 second time steps. Here $S=4\text{m/s}$, believed to be typical of ship speeds in the second half of the nineteenth century. The bucket is assumed to continue to cool from its base throughout the period of exposure while the heat exchanges through the water surface are reduced to 75% of their value for a freely exposed surface. Cooling rates of this bucket are typically 20% of those of the large canvas bucket. Thus a cooling of just over 0.1°C for $u=5\text{m/s}$ at 10m, $K=0.3\text{ Wm}^{-1}\text{ }^{\circ}\text{C}^{-1}$, an air sea temperature difference of -1°C and $\text{RH}=75\%$ (the cooling is about 75% of that shown as a cross) is small, but not entirely negligible.

Figs 7 and 8 show similar curves for $\text{SST}=10^{\circ}\text{C}$ and air temperature $=8^{\circ}\text{C}$ (typical extratropical conditions in winter) for canvas and wooden bucket respectively. Fig. 8, for the wooden bucket, shows curves for two values of K . The lower value of K is about the minimum for dry wood and reduces the cooling rate to about 65% of that using $K=0.3\text{ Wm}^{-1}\text{ }^{\circ}\text{C}^{-1}$ much as for equatorial conditions in Fig 6. The rate of cooling of the canvas or wooden bucket with a given value of K is roughly 40% of that for the same bucket in equatorial conditions (Figs 5 and 6 respectively), showing the importance of evaporation rate in the heat balance. However in winter, air-sea temperature differences and wind speeds are often considerably larger in the extratropics than the tropics. So for the extratropical conditions of Fig. 7, an air-sea temperature difference of -2°C , a wind speed of 10m/s, $S=7\text{m/s}$ and $\text{RH}=75\%$, the large canvas bucket is calculated to cool about 0.35°C after 4 minutes, about 0.15°C less than for the typical equatorial conditions mentioned above. However, for typical December conditions east of Cape Hatteras around 35°N with $\text{SST}=20^{\circ}\text{C}$, air temperature 15°C , 10m wind speed 10m/s, $\text{RH}=75\%$ and $S=7$, cooling after 4 minutes reaches 0.85°C (for an Ashford bucket with $F=1$, cooling exceeds 0.9°C). This is the region and season where bucket corrections are largest (Bottomley *et al.*, 1990).

7.2 Cooling as a function of exposure time

Fig. 9 shows cooling curves for the large canvas bucket for $S=7\text{m/s}$, $\text{RH}=75\%$ for two values of 10m wind speed u , and for the equatorial and extratropical conditions of Figs 5-8. The faster cooling in the first 1.5 minutes is contributed to by the insertion of the thermometer in the third half minute whose temperature is assumed to be that of the air. Tropical conditions clearly give more cooling for a given wind speed. The cooling after 3 minutes exposure time for the equatorial conditions shown when $u=5\text{m/s}$ is about the same as that for the extratropical conditions after 10 minutes exposure time with $u=15\text{m/s}$. In

practice, typical cooling rates in the tropics and the extratropical winter are often comparable due to higher wind speeds and larger air-sea temperature differences in the latter.

Fig. 10 shows the influence of short wave radiation Q (direct and diffuse) on the cooling rate of the canvas bucket. For $Q=100 \text{ Wm}^{-2}$ the decrease in cooling rate compared to $Q=0$ is nearly independent of all other exposure variables. There is a larger fractional decrease in cooling in the extratropics, but even there the effect is only strong second order. Warming effects are likely to be largest in the tropics and in mid-latitude summer as Q would be largest then. So only rough estimates of Q are needed in a correction procedure. If the bucket is shaded the effects of diffuse radiation will be small.

Fig. 11 shows cooling curves for $S=4\text{m/s}$ for the large wooden bucket for up to six minutes exposure time. The curves have a different shape from those for the canvas bucket in Fig. 9. The canvas bucket cooling rate tends to slowly decrease after the insertion of the thermometer at 1.5 minutes exposure time, whereas the wooden bucket rate slowly increases after this. Insertion of the thermometer causes much of the increase in rate in the third half minute. However after 6 minutes the total cooling of the water in the wooden bucket is still only about 20-25% of that of the canvas bucket for the same conditions.

8. On deck tests of the theory of the cooling of a canvas bucket

8.1 Procedure

The following tests were organised by Professor R Newell and carried out by students of the USA Sea Education Association on the deck of a ship in the tropical North Atlantic in February and March 1991. An Ashford type (UK Met Office) canvas bucket was filled with water and the temperature of the water, kept well mixed, was monitored for 10 minutes. The bucket was kept in shade and the ambient temperature and humidity were measured using a whirling psychrometer. The wind speed past the bucket at bucket level was measured with a hand anemometer. As a check, the sea surface temperature was also measured using a plastic bucket and the air temperature taken by the thermistor used to measure the changing bucket temperature just before immersion. The thermistor measurements did not always agree well with those from the whirling psychrometer. For consistency, the whirling psychrometer dry bulb values have been chosen as these were used to calculate the vapour pressure (not surprisingly, the thermistor air temperature values gave slightly less consistent results compared to the theory). Twenty four sets of measurements were analysed (one set being rejected) that covered a range of cooling of the bucket from zero to 1°C in ten minutes. In the model it was assumed that $F=1$.

8.2 Results

Figs 12a-12c show three typical examples of modelled and observed cooling curves covering the range of modelled cooling from slight warming over 10 minutes to a cooling of about 0.8°C . Fig. 12 is typical of the other results: modelled and observed cooling rates agree moderately well but very close correspondence only occurs

FIG 12a TEMPERATURE CHANGE OF SEA WATER
IN MET OFFICE CANVAS BUCKET - example 1
Init. water temp=24.8 deg C, U=2.69 m/s
air temp=21.8 deg C, RH=92.0%.

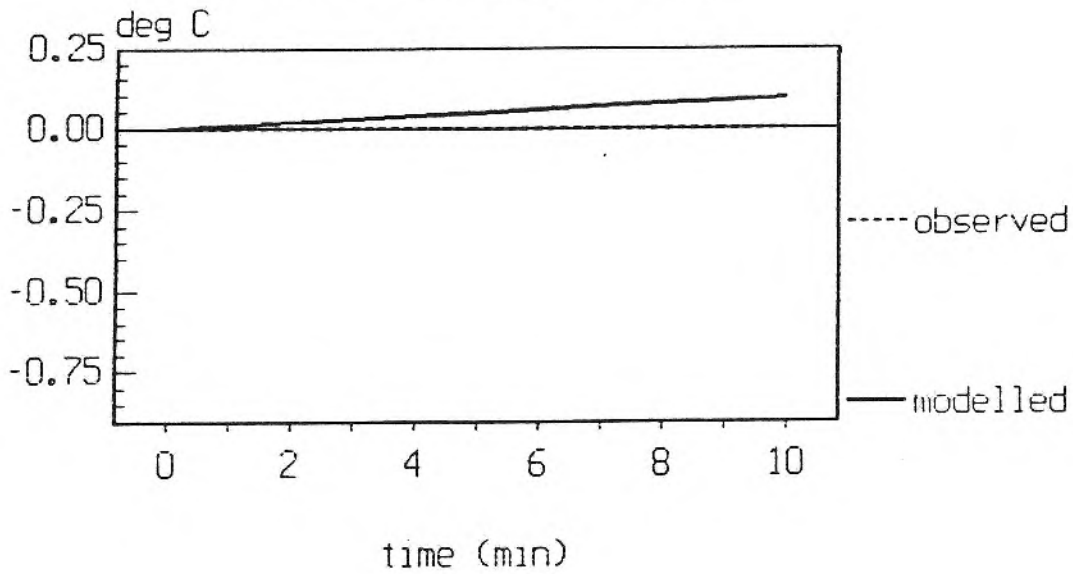


FIG 12b TEMPERATURE CHANGE OF SEA WATER
IN MET OFFICE CANVAS BUCKET - example 2
Init. water temp=26.1 deg C; U=4.93 m/s
air temp=26.1 deg C, RH=88.5%.

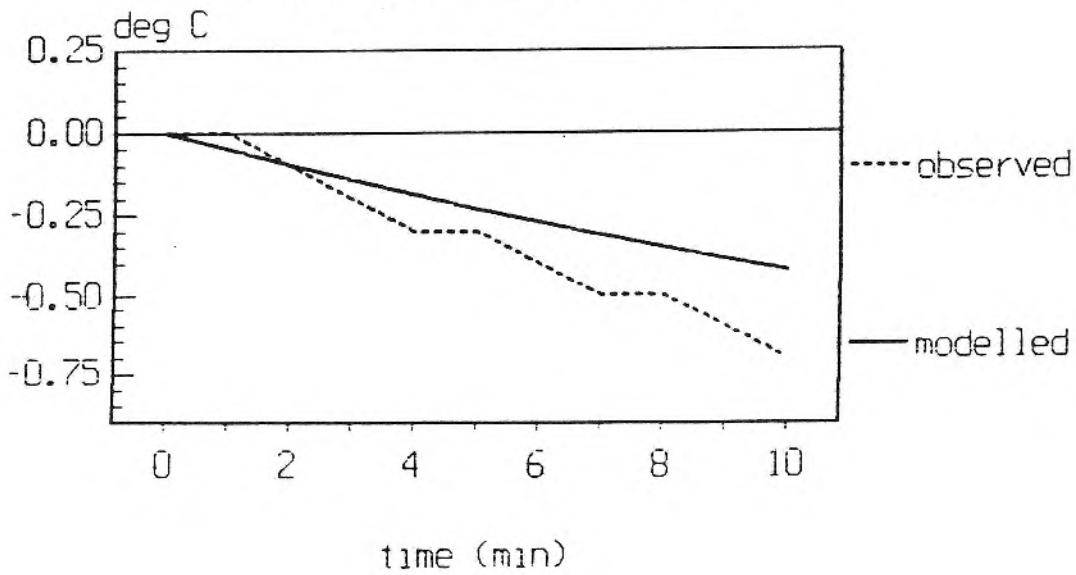


FIG 12c TEMPERATURE CHANGE OF SEA WATER
 IN MET OFFICE CANVAS BUCKET - example 3
 Init. water temp=26.4 deg C, U=5.82 m/s
 air temp=26.8 deg C, RH=77.9%

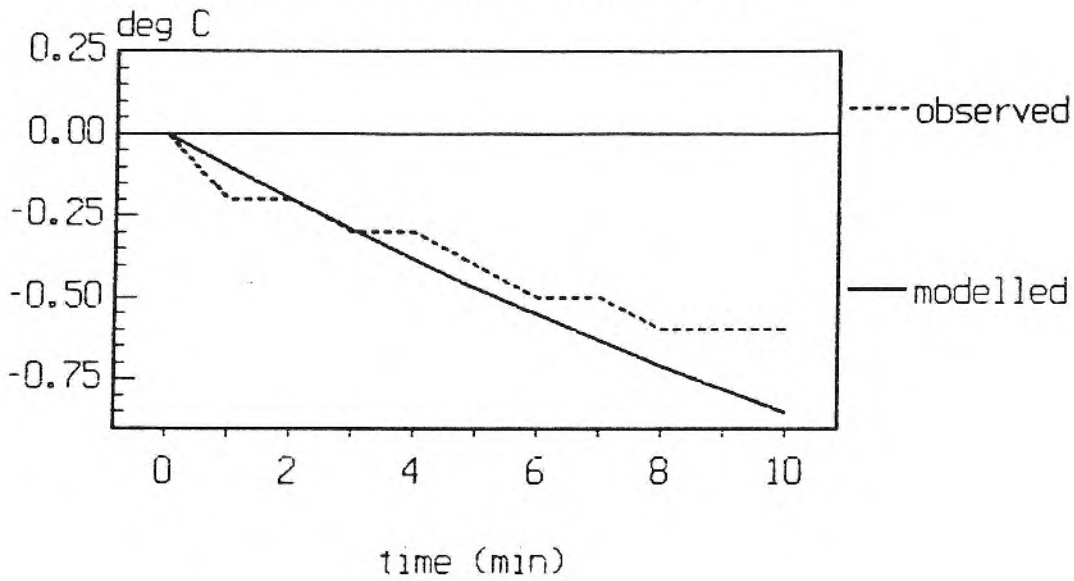
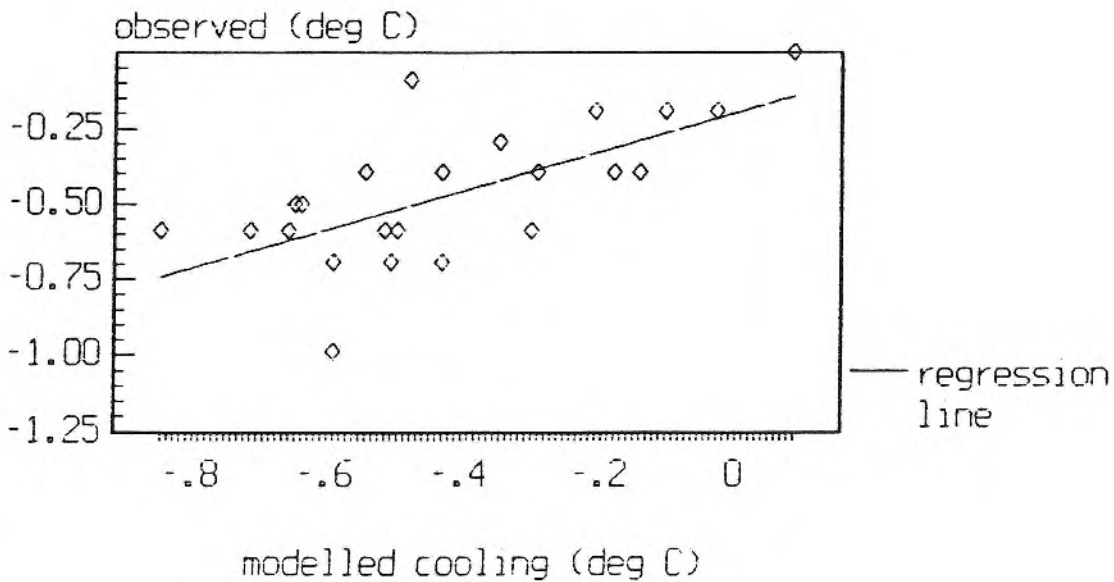


FIG 13 OBSERVED & MODELLED COOLING OF A
 UK MET OFFICE CANVAS BUCKET AFTER 10 MIN
 - all data



in a minority of cases. This is not surprising given the difficulty of making measurements of temperature and wind speed exactly adjacent to the bucket; furthermore the observations of ambient conditions are only single spot values, whereas more frequent values may be desirable during the ten minutes exposure period. Another source of uncertainty concerns the depth of water in the bucket; this was not recorded but attempts were apparently made to fill the bucket. Fig. 12 assumes an initial water depth of 18cm, leaking at a rate of 0.5cm/min.

Over all 24 sets of measurements, the correlation between the total observed and modelled temperature change after 10 minutes was 0.67. The average observed change was -0.46°C and the averaged modelled change was -0.41°C , a mean difference of 0.05°C or 11% of the mean observed temperature change. This difference was not statistically significant according to a t test. Fig. 13 summarises the results. It is tentatively concluded that the model gives about the correct form of cooling curve (Fig. 12) and its overall estimates of cooling rate may be unbiased. Clearly many more on deck data are needed to confirm this conclusion, preferably including more frequent measurements of ambient conditions while the bucket is exposed. As explained in section 3, the most likely error is a modest underestimate of cooling rate if the ambient airflow is turbulent.

8.3 Summary of how bucket models are used to correct historic SST data

As explained in FP(1990), the correction of SST data as made in Bottomley *et al.* (1990) depends on the use of the average of corrections derived from several bucket models in a special way that takes advantage of a remarkable characteristic of historical SST data. We observe that the annual cycle of sea surface temperature away from the equator was considerably larger on average prior to 1942 than afterwards with a sometimes remarkably sudden decrease after 1941. The models are integrated until corrections derived from the calculated cooling or heating in each calendar month gives an annual cycle of SST in pre-1942 data (away from the equator) closest in magnitude to that observed for 1951-80. Near the equator where annual cycles are too small to use, the model is integrated for the same time as in extratropical regions, This allows a global set of 5° calendar monthly corrections to be calculated. Pre-1942 annual cycles in uncorrected SST are largest compared to those for 1951-80 in the North Atlantic and North Pacific between 30 and 50°N ; running the canvas bucket models for a few simulated minutes gives corrections which give the required reduction in the annual cycle. The final set of corrections for each 5° box are averages for each calendar month calculated from several models that use buckets of different size exposed to fixed climatological conditions of wind speed, humidity, temperature etc calculated for 1951-80 over the box. Running the bucket models for too long an exposure time results in an increase in the difference in the size of the annual cycle between pre-1942 and 1951-80 data with altered phase (see FP, 1990). Models run with different bucket sizes and reasonable changes to assumed conditions on deck invariably give similar but not identical sets of corrections. The compensating factor is the length of time that the bucket model needs to be integrated; this is least for small buckets that cool the fastest. For canvas buckets, the range of times

spans those recommended in historical instructions when allowance is made for a bucket hauling phase.

Thus the bucket model correction technique gives results largely independent of factors for which precise details are not known. An exception concerns the sensitivity of the corrections to our lack of knowledge of the mix of wooden and canvas buckets used in the 19th century. This is discussed in FP: different assumptions about the mix of canvas and wooden buckets are a part of the cause of differences in calculated 19th century corrections between FP and FWJS. Differences in the correction procedures for the cooling of wooden buckets and differences in the data are the other causes of different analysed temperature levels.

9. Summary

This note contains the complete theory of the bucket models. The limited tests of the canvas bucket theory on board ship appear to be validate the theory, though further results are needed. The way the models are used to correct SST data is quite fully described in FP(1990); a similar technique used to correct more recent analyses using the latest version of the theory described here will be discussed fully in FP(1992). In FP(1990) the canvas bucket model is similar in form to that used here. However the wooden bucket model is different as discussed in section 6. The biggest problem affecting corrections remains the uncertainty in the changing fraction of wooden and uninsulated buckets used in the nineteenth century.

Acknowledgements

The author is indebted to David Parker who has critically examined the theory and has helped with some practical experiments, and to Professor Reginald Newell and students of the USA Sea Education Association Inc. for organising and carrying out measurements of the cooling of a canvas bucket on board ship. Thanks are due also to Peter Stevenson who wrote most of the original programs used to correct the historical SST data based on the author's PC code.

REFERENCES

- Ashford O.M., 1948. A new bucket for measurement of sea surface temperature. Q. J. Roy. Met. Soc., 74, 99-104.
- Bottomley M., Folland C.K., Hsiung J., Newell R.E. and Parker D.E., 1990. Global Ocean Surface Temperature Atlas "GOSTA". Joint project of the Met Office and Massachusetts Institute of Technology supported by US Dept of Energy, US National Science Foundation and US Office of Naval Research. Publication funded by UK Depts of Environment and Energy for the Intergovernmental Panel on Climate Change. Printed by HMSO, London. 20pp+iv, 313 plates.
- Brooks C.F., 1926. Observing water-surface temperatures at sea. Mon. Wea. Rev., 54, 241-254.

- Eckert E.R.G. and Drake R.M., 1972. Analyses of heat and mass transfer. McGraw-Hill Kogakusha, Tokyo.
- Eckert E.R.G. and Drake R.M., 1985. Introduction to Heat and Mass Transfer. Second Edition. Tata Mcgraw-Hill, New Delhi.
- Farmer G., Wigley T.M.L., Jones P.D. and Salmon M., 1989. Documenting and explaining recent global-mean temperature changes. Climatic Research Unit, Norwich, Final Report to NERC, UK, Contract GR3/6565.
- Folland C.K. and Hsiung J., 1987. Correction of seasonally-varying biases in uninsulated bucket sea surface temperature data using a physical model. Second minor revision, Met O13 Branch Memo 154. Available from the National Meteorological Library, Met Office, Bracknell, Berks, UK, RG12 2SZ.
- Folland C.K., 1988. Numerical models of raingauge exposure, field experiments, and a new collector design. Q. J. Roy. Met. Soc., 114, pp1485-1516.
- Folland C.K., Karl T.R, and Vinnikov K.Ya, 1990. Observed Climate Variability and Change. In: Climate Change, WMO/UNEP Intergovernmental Panel on Climate Change Scientific Assessment, pp195-238. Eds: J.T. Houghton, G.J. Jenkins and J.J. Ephraums. Cambridge University Press.
- Folland C.K. and Parker D.E., 1990. Observed variations of sea surface temperature. In: "Climate-Ocean Interaction" NATO/CEC ARW, Oxford, England, Sept 26-30, 1988, pp21-52. Ed: M. Schlesinger, Kluwer Academic Publishers.
- Folland C.K. and Parker D.E., 1992. A physically-based technique for correcting historical sea surface temperature data. To be submitted to Q. J. Roy. Met. Soc.
- Kaye G.W.C and Laby T.H., 1986. Tables of physical and chemical constants and some mathematical functions. 15th edition. Longman, London. 477pp.
- Maury M.F., 1858. Explanations and sailing directions to accompany the wind and current charts. Vol. 1, 383pp+51 plates. Printed by W.A. Harris, Washington DC.
- Meteorological Office, 1868. Directions for using the instruments. London, 8pp.
- Meteorological Office, 1956. Handbook of meteorological instruments, Part I. MO 577, HMSO, London.
- Parker D.E. and Folland, C.K., 1991. Worldwide surface temperature trends since the mid-19th century. In: M.E.Schlesinger (ed), Greenhouse-Gas-Induced-Climate Change: a Critical Appraisal of Simulations and Observations, pp173-193. Elsevier, Amsterdam.
- Wylie R.G., 1968. Resume of knowledge of the properties of the psychrometer. In: Final Report of the Working Group on Hygrometry, resolution 4, CIMO IV, WMO, Geneva.

$$h_x = 0.33k \left(\frac{\bar{u}_0}{x\nu} \right)^{0.5} Pr^{0.333}$$

Assuming that k , Pr , and ν are constant, with the values shown in the canvas bucket section, we can rewrite the above as:

$$h_x = \beta \left(\frac{\bar{u}_0}{x} \right)^{0.5}$$

where

$$\beta = 0.33k \frac{Pr^{0.333}}{\nu^{0.5}}$$

Substituting this expression for h_x into equation A1.1 and noting that $L=D\sin\theta$ we obtain:

$$\bar{h}_x = 2h_L = 2\beta \left(\frac{\bar{u}_0}{D\sin\theta} \right)^{0.5} \quad (A1.2)$$

Thus the mean heat transfer coefficient along AB is twice that at the leeward end. It remains to find the areas associated with all narrow filaments centred on lines like AB. Consider figure A1.1. The length of line CD is $D/2\cos\theta$ and of line CD' is $D/2(\cos(\theta+d\theta))$. A little manipulation gives the filament width, the difference of these two lengths, as $D/2\sin\theta d\theta$. Now the length $L=D\sin\theta$, giving a filament area of $D^2/2 \sin^2\theta d\theta$. Let this be dA and the area of the base A . Then the mean heat transfer coefficient for the base is given by the mean value of all possible values of $2h_L$ i.e.

$$2\bar{h}_L = \frac{1}{A} \int_0^\pi 2h_L dA$$

$$\text{i.e. } 2\bar{h}_L = 2 \frac{\beta}{A} \left(\frac{\bar{u}_0}{D} \right)^{0.5} \int_0^\pi \frac{dA}{\sin^{0.5}\theta}$$

Substituting for the area of the circular base we get:

$$2\bar{h}_L = h_{base} = 4 \frac{\beta}{\pi} \left(\frac{\bar{u}_0}{D} \right)^{0.5} \int_0^\pi \sin^{1.5}\theta d\theta$$

Substituting $\sin^{1.5}\theta=1.75$, $K=0.025Wm^{-1} \text{ } ^\circ C^{-1}$, $Pr=0.71$ and $\nu=1.5 \times 10^{-5} m^2 s^{-1}$ gives $\beta=1.91 h_{base}$ is:

$$h_{base} = 4.3 \left(\frac{\bar{u}_0}{D} \right)^{0.5} \quad (A1.3)$$

APPENDIX 2

EQUIVALENCE OF THE BUCKET MODEL TO THAT OF THE THEORY OF THE PSYCHROMETER

For simplicity let $Q_s=0$ (the usual situation with a wet bulb). When the canvas bucket temperature is in equilibrium, as with a wet bulb, $dQ/dt=0$. We assume that pure water is being used. Then the loss of heat due to evaporation equals the gain of heat due to sensible and radiative heat transfer in equation 12 (short wave radiation is assumed not to be incident). However first let the factor 1.7 in equation 12 be replaced by a value, 1.72, correct to three significant figures and also recalculated for a pressure of 1000mb as normally used in calculations of the psychrometer coefficient.

$$[h_r(A_{base}+A_{cyl})+h_{cyl}A_{cyl}+h_{base}A_{base}](t_a-t_b)=1.72(h_{cyl}A_{cyl}+h_{base}A_{base})(e_b-$$

If we divide both sides by the factors multiplying e_b-e_a the resulting factor multiplying t_a-t_b is the psychrometer coefficient appropriate to a pressure of 1000mb. Replace suffix b by suffix w to represent a wet bulb. Then for a small narrow bulb with $A_{base} \ll A_{cyl}$ we have:

$$e_w - e_a = 0.58 \left(1 + \frac{h_r}{h_{cyl}} \right) (t_a - t_w) \quad (A2.2)$$

First set $h_r=0$. We obtain, independently of all heat transfer coefficients:

$$e_w - e_a = 0.58 (t_a - t_w) \quad (A2.3)$$

The constant 0.58 is the theoretical value of the psychrometer coefficient, when the influence of long wave radiation is not taken into account, for a surface pressure of 1000mb given by Wylie (1968). When we include h_r , the psychrometer coefficient depends (fairly weakly) on wind speed and, if not very narrow, on the thermometer diameter. So the psychrometer coefficient depends weakly on the details of the cylindrical geometry (equation A2.1). Setting $h_r=5.4Wm^{-2} \text{ } ^\circ C^{-1}$, consider an incident mean wind speed $5ms^{-1}$ and a typical thermometer diameter 0.005m and bulb length 0.03m. Then as $Re>10^3$ we use equation 5d to calculate h_{cyl} . For a surface pressure of 1000mb, we get the larger psychrometer coefficient of 0.62 which is still slightly below the observed value of 0.666 for the probable reasons discussed by Wylie (1968). For a canvas bucket of diameter 16cm, typical

water depth 15cm, air speed of 3ms^{-1} on deck blowing past the bucket, $F=0.25$, and no incident short wave radiation, the "psychrometer coefficient" is 0.76 using equation A2.1.

CLIMATE RESEARCH TECHNICAL NOTES

- CRTN 1 Oct 1990 Estimates of the sensitivity of climate to vegetation changes using the Penman-Monteith equation.
P R Rowntree
- CRTN 2 Oct 1990 An ocean general circulation model of the Indian Ocean for hindcasting studies.
D J Carrington
- CRTN 3 Oct 1990 Simulation of the tropical diurnal cycle in a climate model.
D P Rowell
- CRTN 4 Oct 1990 Low frequency variability of the oceans.
C K Folland, A Colman, D E Parker and A Bevan
- CRTN 5 Dec 1990 A comparison of 11-level General Circulation Model Simulations with observations in the East Sahel.
K Maskell
- CRTN 6 Dec 1990 Climate Change Prediction.
J F B Mitchell and Qing-cun Zeng
- CRTN 7 Jan 1991 Deforestation of Amazonia - modelling the effects of albedo change.
M F Mylne and P R Rowntree
- CRTN 8 Jan 1991 The role of observations in climate prediction and research.
D J Carson
- CRTN 9 Mar 1991 The greenhouse effect and its likely consequences for climate change.
D J Carson
- CRTN 10 Apr 1991 Use of wind stresses from operational N.W.P. models to force an O.G.C.M. of the Indian Ocean.
D J Carrington
- CRTN 11 Jun 1991 A new daily Central England Temperature series, 1772-1991.
D E Parker, T P Legg and C K Folland
- CRTN 12 Jul 1991 Causes and predictability of Sahel rainfall variability.
D P Rowell, C K Folland, K Maskell, J A Owen, M N Ward
- CRTN 13 Jul 1991 Modelling changes in climate due to enhanced CO₂, the role of atmospheric dynamics, cloud and moisture.
C A Senior, J F B Mitchell, H Le Treut and Z-X Li

